PHYSICAL REVIEW B VOLUME 17, NUMBER 6 15 MARCH 1978

Theory of the elastic strain energy due to crystallographic shear plane arrays in reduced rutile (TiO_2)

Yasuhiro Shimizu and Eisuke Iguchi
Department of Metallurgical Engineering, Yokohama National University, Minami-ku, Yokohama, 233 Japan

(Received 1 August 1977)

Calculations of the elastic strain energy due to an infinite ordered array of crystallographic shear (CS) planes lying on {132} and {121} planes in reduced rutile (TiO_2) have been made by using the Fourier-transform treatment. The strain energy per unit area per CS plane and per unit volume for an infinite ordered array have been evaluated as a function of n in Ti_nO_{2n-1}. It was found that, though the strain energy per unit area per {132} CS plane is less than that per {121} plane, there is a crossover in the strain-energy curves per unit volume for the {132} and {121} CS planes. These quantitative results clarify the experimental observations that initial reduction of TiO_2 results in randomly distributed CS planes upon {132} planes and the change from {132} to {121} shear planes takes place as the oxygen deficiency is increased. The stability of members of the homologous series of oxides, Ti_nO_{2n-1}, has been discussed by comparing the strain energy in a crystal of an oxide Ti_nO_{2n-1} with that in a crystal containing two phases, $Ti_{n-1}O_{2(n-1)-1}$ and $Ti_{n+1}O_{2(n+1)-1}$. The calculated results agree well with the microstructures of CS-plane arrays observed in practice and it was found that the elastic strain energy plays a significant role in controlling the microstructure of a crystal containing CS planes.

I. INTRODUCTION

A great deal of work has been carried out concerning the nonstoichiometry in rutile (TiO_2).[1] In particular the correlation between the physical properties and the structure of point defects supposed to exist in slightly reduced rutile has been investigated in detail.[2–6] On the other hand, it has been established that at greater degrees of reduction than about $TiO_{1.998}$ the change in anion to cation stoichiometry is accounted for by the formation of crystallographic shear (CS) planes[7] and it is by no means certain that concentrations of point defects above the thermodynamic requirement of Schottky and Wagner statistics exists in TiO_x.

The structures of CS planes in reduced rutile have been investigated fairly thoroughly on the basis of solid-state chemistry and a reasonable amount of precise information on the crystal chemistry of these CS structures is available. These show that when rutile is reduced to composition $TiO_{1.98}$ to $TiO_{1.93}$, the CS planes lie upon {132} planes ({132} CS planes) and a homologous series of compounds, Ti_nO_{2n-1}, with $n = 16–36$ is formed. These {132} CS planes were indexed by using a series of electron-diffraction patterns[8,9] which showed that unambiguous indexing was only possible for $n \leq 22$ revealing only *even* values of n. A considerable number of patterns clearly demonstrated that, in "two-phase" mixtures, $\Delta n = 2$. These observations suggest that *even*-n values are also favored for $n > 22$.[8,9]

In the region $1.66 \leq x (\text{in } TiO_x) \leq 1.90$, Andersson *et al.*[7,10–12] showed that a homologous series of oxides, Ti_nO_{2n-1}, based upon {121} CS planes is formed with n of 4–10. Later Terasaki and Watanabe observed the homolog $n = 10$ though it was coexisted with other homologs.[13]

In the intermediate-composition range $1.89 \leq x \leq 1.93$, an ordered phase forms. The CS planes have an index between {121} and {132}, but they are ordered. This is the swinging CS-plane region.[9,14] According to Bursill and Hyde, the transition from a {132} to a {121} CS plane is expected to take place through the progression {132} → {253} → {374} → {495} · · · → {121} and they observed ordered {253} arrays experimentally.[14]

When rutile is reduced slightly ($1.998 \leq x \leq 2.00$), besides point defects, {011} antiphase boundaries or {132} CS planes are formed.[8] In this region, {132} CS planes are randomly distributed or tend to cluster in pairs or in groups. Some parts in large clusters are found to have structures corresponding to the ordered array with $n = 37$.[15]

Despite such an amount of information on the crystal chemistry of CS structures, there are only a few papers in which the nature of CS planes has been treated quantitatively on the basis of solid state physics.[16–19] Unfortunately, most of these studies are concerned with reduced tungsten trioxide. Thus, in an attempt to analyze the large amount of information concerning the microstructures of CS phases, several authors have attempted to assess the strain energy caused by the defect forces within CS planes.[16,17] Stoneham and Durham[16] calculated the strain energies of the infinite ordered array and a pair of {001} CS planes in a ReO_3-type crystal by the use of Fourier transformation and found the equilibrium separations of the planes which were most stable. Iguchi and Tilley[17] computed the strain energies in the matrix between CS planes in reduced WO_3. Though their calculation is complicated because they have not employed the Fourier-transform method, their treatments can be applied to not only the ordered arrays but also to other plausible distributions of CS planes.

These theoretical studies have made progress in a quantitative understanding of CS structures in reduced WO_3. In this report, however, we will evaluate, using the Fourier-transform treatment, the strain energy due to $\{132\}$ and $\{121\}$ CS planes which are the typical ones in reduced rutile and have much more complicated crystallographic structures than CS planes in reduced WO_3. Then we will consider the relevance of the elastic strain energy to the CS geometries observed in practice. According to Clapp's analysis,[20] the configurational entropy appears to be quite negligible, so the internal energy proves to be the important part of the free energy and the major internal energy is likely to come from elastic strain. Many groups have calculated the energies due to lattice defects in crystals. In oxides, Dienes *et al.*[21] and Catlow[22] evaluated the formation energies and migration energies of point defects. On the other hand, in metals, Kanzaki,[23] Khachaturyan,[24] Cook *et al.*,[25] and Hoffman[26] employed the discrete-lattice model and expanded very complicated theories. In this paper, we have simplified the theoretical treatment as much as possible by using the elastic-continuum theory and the elastic Green's function.

II. THEORY

The microstructure of a crystal containing CS planes changes as the degree of reduction varies, as described in Sec. I. The interaction between CS planes may provide a key to understanding these microstructures and so we attempt to evaluate them here. The terms considered to contribute to the interaction are the following. First, there is the strain energy in the crystal, parts of which have been calculated by Stoneham *et al.*[16] and Iguchi *et al.*[17]; second, we have the electrostatic interaction between ions in the CS plane and in the matrix and the repulsive Coulomb energy between CS planes, if they are not neutral[18]; third, the polarization effect is a very important factor as well because the CS planes seem only to be formed in oxides which have high dielectric constants.[18]

Among these factors, as Anderson suggested,[27] the strain energy must be surely one of the most dominant factors. Iguchi and Tilley made an estimate of the electrostatic interaction energy between ions in CS planes and in the matrix and found it to be negligible compared with the strain energy.[18] Although the polarization terms should be present, it seems hard at present to treat this effect theoretically[28-30] and so this will be postponed to the future.

The strain energy can be regarded as consisting of the following two parts. One is the strain energy in the matrix caused by defect forces in the CS planes and the other is the interaction energy between a defect force and all other defect forces in the crystal. The latter is written as the scalar product of the force acting on a cation in a CS plane with the displacement of this ion due to all other forces. Then, if the cation displaces along the defect force acting on it, this interaction helps to counteract the increase in the elastic strain energy, which implies that this is a relaxation energy. Hence this idea is similar to that of Stoneham *et al.*[16] Here we denote the strain energy in the matrix and the relaxation energy as E_S and E_R, respectively; then, the interaction energy in the crystal induced by CS planes E_I can be given as follows: $E_I = E_S - E_R$. We will evaluate the energy E_I for infinite ordered $\{132\}$ and $\{121\}$ arrays. In calculating the strain energy E_S in the discrete-lattice model,[23-26] the defect forces could be, in principle, obtained from a detailed study of the local strain near isolated point defects. However, the local strain around CS planes looks difficult to be estimated precisely at present. So we have evaluated the ion displacements using the elastic Green's function by which means the equilibrium between the defect forces and the ion displacements can be obtained when the point-defect forces work in the elastic continuum. In this treatment, information about the detailed ionic positions is not necessary and, moreover, the displacement and the strain at any position can be calculated only if the defect forces which give rise to the deformation of the continuum are hypothesized properly. How to determine defect forces will be described in Sec. II B. Therefore, the strain energy in this report is not given by the scalar product of the displacements of each ion as in the discrete-lattice model, but is represented in terms of the strain energy density ω. By using the elastic-continuum model, we can remove such complicated treatments of the discrete-lattice model, but we have to accept some assumptions which will be described later.

A. Structure of $\{132\}$ and $\{121\}$ CS planes

In Fig. 1, a clinographic projection of the rutile structure is shown. The rutile structure consists

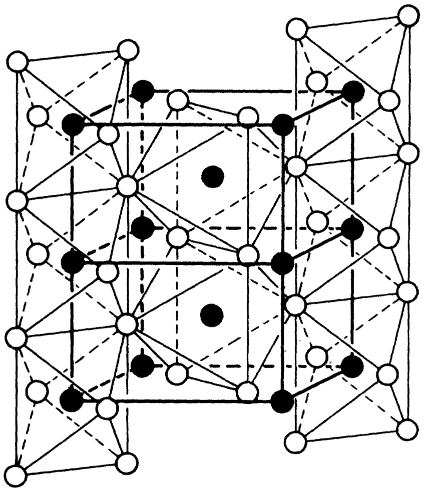

FIG. 1. Clinographic projection of the rutile structure. Two unit cells are heavily outlined. The lightly outlined (TiO_6) octahedra are connected by edges to give ribbons which are in turn connected by corners. Closed circles, Ti; open circles, O. Every Ti ion is located at the body-centered site of the (TiO_6) octahedron.

of rectilinear ribbons of edge-shared (TiO_6) octahedra joined by corner-sharing to similar ribbons so that the orientations of adjacent ribbons differ by $\frac{1}{2}\pi$ rad. The heavily outlined cells in Fig. 1 are tetragonal, Ti ions are located at the corner (0, 0, 0) and at the body-centered site $(\frac{1}{2}, \frac{1}{2}, \frac{1}{2})$ of the unit cell. The oxygen ions are located at $\pm(u, u, u)$ and $\pm(\frac{1}{2}+u, \frac{1}{2}-u, \frac{1}{2})$, where u is estimated to be 0.305,[31] or 0.306.[32] In order to simplify the theoretical treatment as much as possible, however, we have used the idealized relation, $u=0.25$, by which we can construct the idealized structure that Anderson and Hyde employed in their geometrical treatment of CS planes in TiO_2.[33] In this structure, the crystal planes normal to $\vec{a}_r$ are constructed by repeating the four layers $Ti(\vec{0})$, $O_2(\frac{1}{4}\vec{a}_r)$, $Ti(\frac{2}{4}\vec{a}_r)$, $O_2(\frac{3}{4}\vec{a}_r)$ as shown in Fig. 2, where subscript r denotes indices based on the rutile cell and the vectors $\vec{a}_r$, $\vec{b}_r$, and $\vec{c}_r$ indicate the unit vectors along the a, b, and c axes of the tetragonal unit cell.

In order to make {132} and {121} CS planes, oxygen ions upon {132} and {121} planes in the perfect crystal are to be eliminated and then these vacant sites allow the formal geometrical collapse operation $(121)\frac{1}{2}[0\bar{1}1]$ and $(132)\frac{1}{2}[0\bar{1}1]$ where (121) and (132) represent the crystal planes and $\frac{1}{2}[0\bar{1}1]$ shows the shear vector. After these operations, {132} and {121} CS planes are formed, the Ti layers of which are indicated in Fig. 3. The sites of oxygen ions do not change relatively to each other before and after the shear operation $\frac{1}{2}[0\bar{1}1]$, so we have omitted the oxygen ions in Fig. 3, but one finds that the spacings between cations in CS planes are reduced compared with the spacings in the idealized structure.

The translation vector from the position of Ti ions in the $Ti(\vec{0})$ layer on the {100} plane shown in Fig. 3 to the Ti sites in the $Ti(\frac{2}{4}\vec{a}_r)$ layer is $\frac{1}{2}(\vec{a}_r - \vec{b}_r + \vec{c}_r)$ and the distribution of Ti ions in the $Ti(\frac{2}{4}\vec{a}_r)$ layer is the same as that in the $Ti(\vec{0})$ layer. Every Ti ion marked with the double circle in the (001) plane shown in Fig. 3 has an adjacent Ti ion in a (200) or $(\bar{2}00)$ plane, the spacing between them being $\frac{1}{2}|\vec{a}_r|$, and the TiO_6 octahedron of the Ti ion marked with the double circle in the (001) plane shares a face with the octahedron of the Ti ion in the (200) or $(\bar{2}00)$ plane. In Figs. 4(a)–4(c), we have shown the Ti sites of the infinite ordered array of CS planes projected on to the (100) plane. As seen in these figures, every array of TiO_6 octahedra which bridges two adjacent CS planes has $\frac{1}{2}n$ octahedra in the case of {132} CS planes with *n even* and, in the case of *odd n* values, the array of $\frac{1}{2}(n-1)$ octahedra and the array of $\frac{1}{2}(n+1)$ octahedra are ordered alternately. On the other hand, there are n octahedra in an array between adjacent {121} CS planes.

The periodic unit cell in the infinite ordered array of CS planes is constructed with the vector $\vec{A}$, $\vec{B}$, and $\vec{C}$, the projection of the unit cell in the (100) plane being outlined heavily in Fig. 4. The vectors $\vec{A}$, $\vec{B}$, and $\vec{C}$ are expressed by linear combinations of the primitive translation vectors $\vec{a}$, $\vec{b}$, and $\vec{c}$ of the idealized rutile structure as

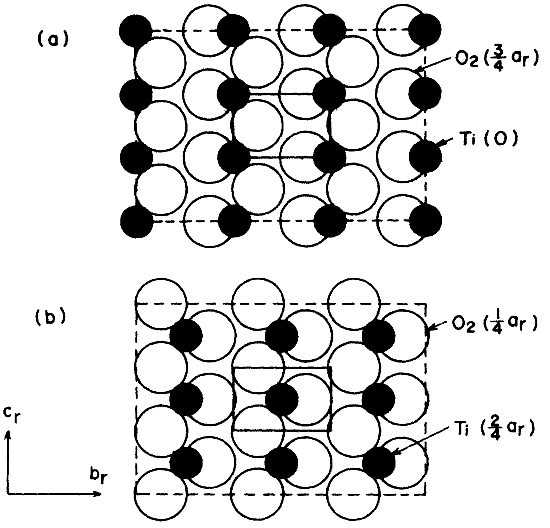

FIG. 2. (100) planes of the idealized structure in which the oxygen sites are represented by the relation $u=0.25$. Closed circles, Ti; open circles, O. (a) $Ti(\vec{0})$ layer and $O_2(\frac{3}{4}\vec{a}_r)$ layer [equal to the $O_2(-\frac{1}{4}\vec{a}_r)$ layer]. (b) $Ti(\frac{2}{4}\vec{a}_r)$ layer and $O_2(\frac{1}{4}\vec{a}_r)$ layer. The unit cell is represented by the solid line. The broken lines in (a) and (b) indicate the same region of the crystal.

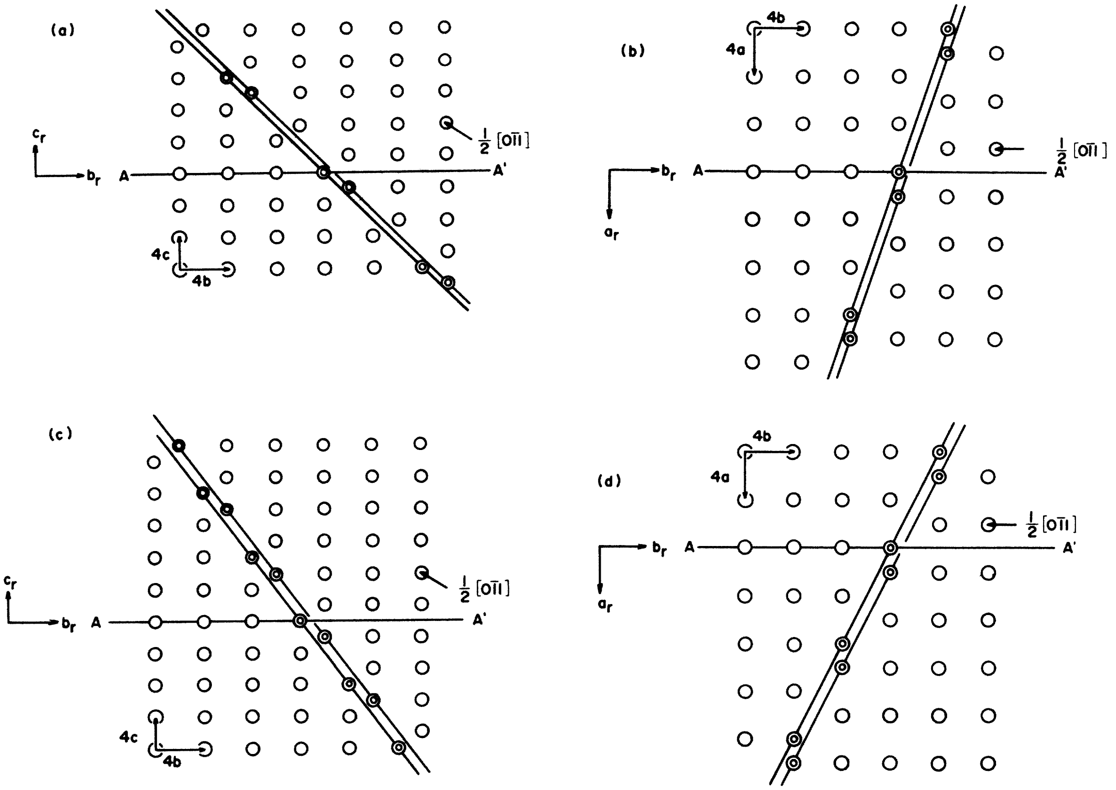

FIG. 3. Ti sites on (100) and (001) planes of the idealized structure. (a) and (b) $(132)\frac{1}{2}[0\bar{1}1]$ CS planes; (c) and (d) $(121)\frac{1}{2}[0\bar{1}1]$ CS planes. Open circles indicate Ti ions. The Ti ion marked with the double circle in (001) has an adjacent Ti ion in (200) or $(\bar{2}00)$ marked also with a double circle and TiO_6 octahedra of these Ti ions share a face with each other. The arrow indicates the $\frac{1}{2}[0\bar{1}1]$ shear vector. The double lines which link centers of double circles represent the core of the CS plane. The cross section normal to (100) along the line *AA'* in (a) is (b) and the cross section normal to (001) along the line *AA'* in (b) is (a). The relation between (c) and (d) is the same. The primitive translation vectors $\vec{a}$, $\vec{b}$, and $\vec{c}$ are also indicated for reference.

follows:

$$\left.\begin{aligned}\vec{A}&=4(\vec{a}-\vec{b}+\vec{c})\\ \vec{B}&=4(2\vec{b}-3\vec{c})\\ \vec{C}&=d_{132}(\vec{b}+\vec{c})\end{aligned}\right\}\text{ for }\{132\}\text{ CS,}\tag{1a}$$

$$\left.\begin{aligned}\vec{A}&=4(\vec{a}-\vec{b}+\vec{c})\\ \vec{B}&=4(\vec{b}-2\vec{c})\\ \vec{C}&=d_{121}(\vec{b}+\vec{c})\end{aligned}\right\}\text{ for }\{121\}\text{ CS.}\tag{1b}$$

Here d_{132} or d_{121} is proportional to the spacing of {132} or {121} CS planes in TiO_2 and is related to n by

$$d_{132}=\tfrac{2}{5}(2n-1),\quad d_{121}=\tfrac{2}{3}(2n-1).\tag{2}$$

The primitive translation vectors $\vec{a}$, $\vec{b}$, and $\vec{c}$ can be expressed in terms of $\vec{a}_r$, $\vec{b}_r$, and $\vec{c}_r$ in the following way:

$$\vec{a}=\tfrac{1}{4}\vec{a}_r,\quad \vec{b}=\tfrac{1}{4}\vec{b}_r,\quad \vec{c}=\tfrac{1}{4}\vec{c}_r,\tag{3}$$

which allows the site of the ions in the idealized structure to be repeated under the translation $\vec{a}$, $\vec{b}$, and $\vec{c}$.

The CS structure of an infinite ordered array of CS planes can be constructed by the formal geometrical transformation $\vec{T}$,

$$\vec{T}=n_1\vec{A}+n_2\vec{B}+n_3\vec{L},\tag{4}$$

where n_1, n_2, and n_3 are integers and $\vec{L}$ is the vector indicated in Fig. 4 and given by Eq. (5),

$$\vec{L}=2(\delta\vec{b}+2L\vec{c}),\tag{5}$$

$$\left.\begin{aligned}&\delta=(-1)^{n+1},\\ &L=\begin{cases}\tfrac{1}{2}(n+1), & n\ \mathit{even}\\ \tfrac{1}{2}(n-2), & n\ \mathit{odd}\end{cases}\end{aligned}\right\}\text{ for }\{132\}\text{ CS,}\tag{6}$$

$$\left.\begin{aligned}&\delta=1\\ &L=\tfrac{1}{2}(2n-3)\end{aligned}\right\}\text{ for }\{121\}\text{ CS.}\tag{7}$$

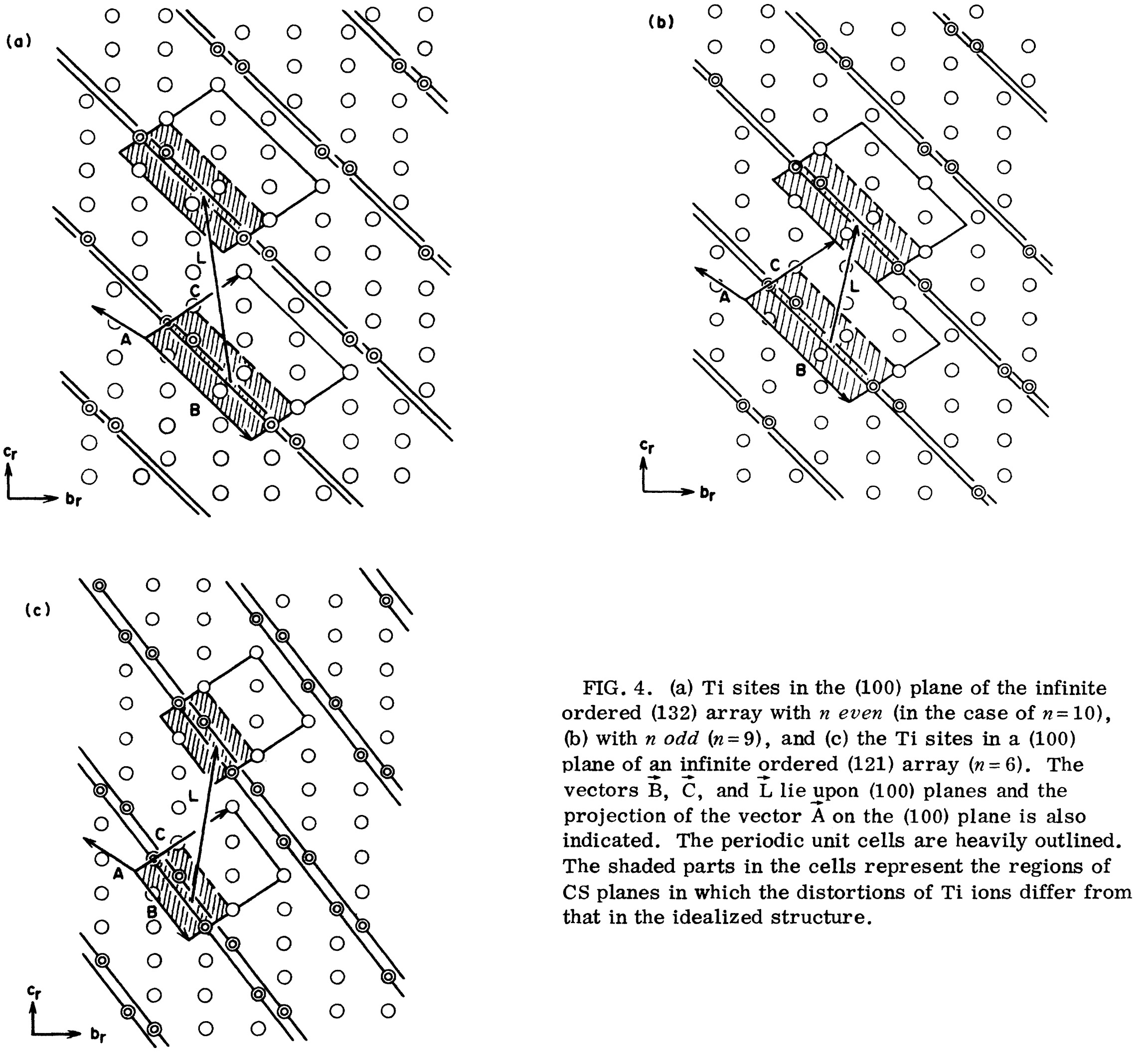

FIG. 4. (a) Ti sites in the (100) plane of the infinite ordered (132) array with *n even* (in the case of $n = 10$), (b) with *n odd* ($n = 9$), and (c) the Ti sites in a (100) plane of an infinite ordered (121) array ($n = 6$). The vectors $\vec{B}$, $\vec{C}$, and $\vec{L}$ lie upon (100) planes and the projection of the vector $\vec{A}$ on the (100) plane is also indicated. The periodic unit cells are heavily outlined. The shaded parts in the cells represent the regions of CS planes in which the distortions of Ti ions differ from that in the idealized structure.

B. Defect forces in CS planes responsible for the strain energy in the crystal

Here we consider the defect forces responsible for the strain in the crystal. From Figs. 3 and 4, it can be seen that in the CS planes, the cations are brought closer together than in the matrix, while the spacing between anions is insensitive to the $\frac{1}{2}[0\bar{1}1]$ shear operation. If we assume an ionic structure for the CS plane, the major forces will be ones of repulsion between cations in the CS plane. Similar defect forces were hypothesized in the CS structure of the W-O binary system,[17,19] which were justified in the experiment by DeAnglis *et al.*[34] using x-ray photoelectron spectroscopy.[20] According to Pauling[35] and Torrens,[36] the interatomic force between ion *i* and *j* can be approximately expressed as

$$f^{q_i,q_j} = q_i q_j e^2/\epsilon r^2 + A\,B\exp(-Br)\,, \qquad (8)$$

where q_i and q_j denote the charges of ion *i* and *j*, and *r* is the separation of these ions, ϵ is the dielectric constant in the matrix between ions, *e* is the unit of the electronic charge, and *A* and *B* are constant terms. Unfortunately, we have no information on the charge state of ions in CS planes, so in this report we have assumed each CS plane to be electrically neutral overall. Although we can have many examples of ionic distribution in CS planes, the following arbitrary arrangement is employed. The valence of Ti ions in the face-shared TiO_6 octahedra is assumed to be $+3e$ and other Ti ions in CS planes have valence $+4e$.

Using these conditions, the forces shown in Fig. 5 are estimated as follows:

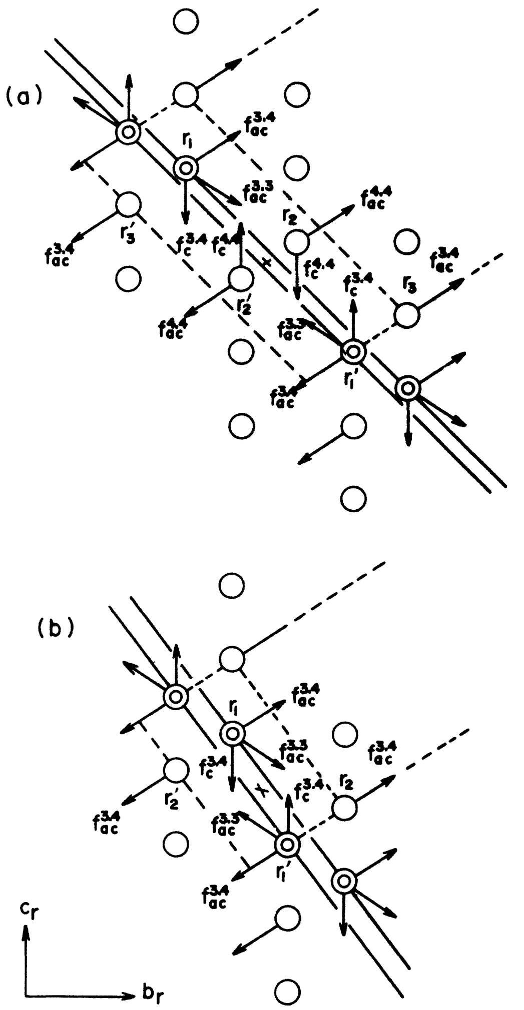

FIG. 5. Defect forces in CS planes projected onto (100). (a) (132) CS plane; (b) $(\bar{1}21)$ CS plane. The force $f_a^{3,3}$ acting on the Ti ion at $\vec{r}_1$, marked with the double circle, is normal to (100) and along [100]. Also $f_a^{3,3}$ on Ti at $\vec{r}_1'$ is normal to (100) and along $[\bar{1}00]$. The origin of the coordinates is taken to be midway between $\vec{r}_1$ and $\vec{r}_1'$.

$$f_a^{3,3}:f_{ac}^{3,3}:f_{ac}^{4,4}:f_{ac}^{3,4}:f_c^{4,4}:f_c^{3,4} \simeq 14.30:3.10:3.27:3.18:1.53:1.45\,. \quad (9)$$

We have used the following values in this estimate[36,37]:

$$A = 9352.6 \text{ (eV)}\,,$$

$$B = 3.5981\ (\text{Å}^{-1})\,,$$

$$\epsilon = \begin{cases} 89.8 \text{ (along } \vec{a}_r), \\ 166.7 \text{ (along } \vec{c}_r), \\ 128.3 \text{ (along } \langle 011 \rangle). \end{cases}$$

Here the average value of the dielectric constants along $\vec{a}_r$ and $\vec{c}_r$ is used as the value in the $\langle 011 \rangle$ direction since we have no data for it. Also, we have employed the following lattice constants[31]:

$$a = 4.5937 \text{ Å}, \quad c = 2.9581 \text{ Å}.$$

In Eq. (9), f_a indicates the repulsive force along $\vec{a}_r$ between Ti ions in the face-shared octahedra, f_{ac} denotes the repulsive force along $\langle 011 \rangle$ between cations in the $\{100\}$ plane, and f_c means the repulsive force along $\vec{c}_r$ acting on a cation in the $\{100\}$ plane which is induced by the asymmetrical distribution of the surrounding cations. In estimating the defect forces, besides the cations described just above, the cations which are located farther away from the CS plane should be considered, but the biggest defect force due to these cations is 0.12, which is very small in comparison with the ratios 14.30–1.45 in Eq. (9). So we have neglected the contribution from these cations. Despite this, estimating the defect forces by using Eq. (8) is rather crude. In order to assess the real defect forces, the long-range forces coming from all other ions in the lattice, e.g., the polarization term as described before and the Madelung term, may be considered as did Dienes *et al.*[21] and Catlow.[22] We have also tried several other plausible models for both the defect forces and the charge distribution associated with the planes, the calculated results are almost similar to the result obtained by using the model in Eq. (9), as will be discussed in some detail later.

C. Strain energy in the matrix due to an ordered array of CS planes E_S

The defect forces in the CS plane induce strain in the matrix. When a unit-volume element deforms reversibly by the different strain increment de_{ij}, the strain energy-density function is obtained by the integration of the work that the stress does on the element, i.e.,

$$\omega = \int \sigma_{ij}\, de_{ij} = \tfrac{1}{2} C_{ijhl} e_{ij} e_{hl}\,, \quad (10)$$

where C_{ijhl} is the elastic constant in tensor form. Thus the strain energy density for a tetragonal elastic continuum has the form[38]

$$\omega = \tfrac{1}{2}\left[C_{11}(e_{11}^2 + e_{22}^2) + C_{33} e_{33}^2\right] + C_{12} e_{11} e_{22} + C_{13}(e_{22} e_{33} + e_{33} e_{11}) + 2C_{44}(e_{23}^2 + e_{31}^2) + 2C_{66} e_{12}^2\,. \quad (11)$$

The displacement in the αth direction of ion at $\vec{r}$, $u_\alpha(\vec{r})$, caused by the βth component of the force at $\vec{r}'$ in a CS plane $F_\beta(\vec{r}')$ is given by the following equation[39]:

$$u_\alpha(\vec{r}) = \sum_{\vec{r}'} \sum_{\beta} G_{\alpha\beta}(\vec{r}-\vec{r}')F_\beta(\vec{r}') \,. \tag{12}$$

In an infinite ordered array, the forces as hypothesized in Fig. 5 repeat periodically, so we can employ the Fourier-transformation treatment. The transformed defect force and Green's function can be written

$$F_\beta(\vec{r}') = \frac{1}{N}\sum_{\vec{q}} \tilde{F}_\beta(\vec{q})e^{-i\vec{q}\cdot\vec{r}'} \,, \tag{13a}$$

$$G_{\alpha\beta}(\vec{r}-\vec{r}') = \frac{1}{N}\sum_{\vec{q}} \tilde{G}_{\alpha\beta}(\vec{q})e^{-i\vec{q}\cdot(\vec{r}-\vec{r}')} \,, \tag{13b}$$

where N is the number of unit cells.[16] We can obtain $u_\alpha(\vec{r})$ by substituting Eq. (13) into Eq. (12):

$$u_\alpha(\vec{r}) = \frac{1}{N}\sum_{\vec{q}} e^{-i\vec{q}\cdot\vec{r}} \sum_{\beta} \tilde{G}_{\alpha\beta}(\vec{q})\tilde{F}_\beta(\vec{q}) \,. \tag{14}$$

The hkth component of the strain e_{hk} is related to the component of the displacement by the following equation:

$$e_{hk} = \frac{1}{2}\left(\frac{\partial u_h}{\partial x_k} + \frac{\partial u_k}{\partial x_h}\right) ; \tag{15}$$

so e_{hk} at $\vec{r}$ in the matrix is given by

$$e_{hk}(\vec{r}) = -\frac{i}{2N}\sum_{\vec{q}} e^{-i\vec{q}\cdot\vec{r}} \sum_{\beta} [q_k\tilde{G}_{h\beta}(\vec{q}) + q_h\tilde{G}_{k\beta}(\vec{q})]\tilde{F}_\beta(\vec{q}) \,. \tag{16}$$

We have assumed that the total strain energy E_S in one periodic unit cell is given as

$$E_S = \sum_{\vec{r}} (\tfrac{4}{3}\pi r_{\vec{r}}^3)\omega(\vec{r}) \,, \tag{17}$$

where $\sum_{\vec{r}}$ indicates the summation of the strain energies of all ions in a periodic unit cell, $\omega(\vec{r})$ denotes the strain energy density of an ion at $\vec{r}$, the ionic radius of this ion being abbreviated as $r_{\vec{r}}$. Since linear elastic theory is used, theoretically one should obtain the unit-cell volume instead of the ionic volume in Eq. (17). The rutile structure, however, consists of edge-shared TiO_6 octahedra as mentioned in Sec. I and has chains of voids called open channels. The volume of voids is nearly equal to the volume of ions. Thus, in order to remove the overestimation on the strain energy E_S, we have made the assumption which is represented by Eq. (17).

D. Relaxation energy E_R

On a cation at $\vec{r}'$ in a CS plane, the defect force $F_\alpha(\vec{r}')$ does work. The displacement of this cation $u_\alpha(\vec{r}')$ induced by another force $F_\beta(\vec{r}'')$ at $\vec{r}''$ can be expressed in a fashion similar to Eq. (12):

$$\begin{aligned} u_\alpha(\vec{r}') &= \sum_{\vec{r}''}\sum_{\beta} G_{\alpha\beta}(\vec{r}'-\vec{r}'')F_\beta(\vec{r}'') \\ &= \frac{1}{N}\sum_{\vec{q}} e^{-i\vec{q}\cdot\vec{r}'} \sum_{\beta} \tilde{G}_{\alpha\beta}(\vec{q})\tilde{F}_\beta(\vec{q}) \,. \end{aligned} \tag{18}$$

Then the total relaxation energy E_R in a periodic unit cell has the form

$$E_R = \frac{1}{N}\sum_{\vec{r}'}\sum_{\alpha} F_\alpha(\vec{r}') \sum_{\vec{q}} e^{-i\vec{q}\cdot\vec{r}'} \tilde{G}_{\alpha\beta}(\vec{q})\tilde{F}_\beta(\vec{q}) \,, \tag{19}$$

where $\sum_{\vec{r}'}$ means the summation of the relaxation energies of all ions in the cell.

Though, in the discrete-lattice model,[24–26] the relaxation energy E_R is twice as large as the strain energy in the matrix E_S, it seems quite difficult in this paper to relate Eq. (17) to Eq. (19). Even if these equations could be combined, a simple relation as the one which is obtained in the discrete-lattice model might never be expected because of the complicated form of Eq. (17).

III. CALCULATIONS AND RESULTS

The defect forces associated with each shear plane in the array have the translation symmetry of the plane itself. The forces repeat under the translation $\vec{T}$ and all transforms $\tilde{F}(\vec{q})$ of the forces in Eq. (13) vanish unless $\vec{q}$ reflects this translation. Then each component of the wave vector $\vec{q}$ can be written

$$\left.\begin{aligned} &\vec{q} = (q_x, q_y, q_z) \,, \\ &q_x = (2\pi/a)[1/(4L+3\delta)][(4L+3\delta)M + (2L+\delta)N + 2P] \\ &q_y = (2\pi/a)[1/(4L+3\delta)](2LN+6P) \\ &q_z = (2\pi/c)[1/(4L+3\delta)](-\delta N+4P) \end{aligned}\right\} \text{ for } \{132\} \text{ CS,} \tag{20a}$$

$$\left.\begin{aligned} &q_x = (\pi/a)[1/(L+1)][2(L+1)M + (2L+1)N + 2P] \\ &q_y = (\pi/a)[2/(L+1)](LN+2P) \\ &q_z = (\pi/c)[1/(L+1)](-N+2P) \end{aligned}\right\} \text{ for } \{121\} \text{ CS,} \tag{20b}$$

where M, N, and P are integers.

The strain energy can be obtained as a sum over discrete values of $\vec{q}$ in the first Brillouin zone of the lattice, i.e, $-4\pi/a \leq q_x,\ q_y < 4\pi/a$, and $-4\pi/c \leq q_z < 4\pi/c$.

A. Fourier-transformed force $\tilde{F}(\vec{q})$

Besides the cations shown in Fig. 5, a periodic unit cell has cations which are translated from the cation in Fig. 5 by $\frac{1}{2}\vec{A}$. In addition, as shown in Fig. 5, in a periodic unit, the force at $\vec{r}'$, $F(\vec{r}')$, and the force at $\vec{r}$, $F(\vec{r})$, are reversed with respect to one another, although they have the same magnitude. We have chosen the origin of the coordinates to be midway between these forces, to give the following relations:

$$F(\vec{r}') = -F(\vec{r}), \quad \vec{r}' = -\vec{r}. \tag{21}$$

Then the Fourier-transformed $\tilde{F}(\vec{q})$ is given as

$$\begin{aligned} \tilde{F}(\vec{q}) &= (1+\cos\pi M)\left(\sum_{\vec{r}} F(\vec{r})e^{i\vec{q}\cdot\vec{r}} + \sum_{\vec{r}'} F(\vec{r}')e^{i\vec{q}\cdot\vec{r}'}\right) \\ &= 2i(1+\cos\pi M)\sum_{\vec{r}} F(\vec{r})\sin(\vec{q}\cdot\vec{r}). \end{aligned} \tag{22}$$

The defect forces and the sites at which they operate are then:

for {132} CS,

site $\vec{r}$	force $F(\vec{r})$
$\frac{1}{4}(0,5,-3)$	$(0, f_{ac}^{3,4}\cos\vartheta, f_{ac}^{3,4}\sin\vartheta)$,
$\frac{1}{4}(0,1,1)$	$(0, f_{ac}^{4,4}\cos\vartheta, f_{ac}^{4,4}\sin\vartheta - f_c^{4,4})$,
$\frac{1}{4}(0,-3,5)$	$(f_a^{3,3}, (f_{ac}^{3,4}+f_{ac}^{3,3})\cos\vartheta,$ $(f_{ac}^{3,4}-f_{ac}^{3,3})\sin\vartheta - f_c^{3,4})$;

for {121} CS,

site $\vec{r}$	force $F(\vec{r})$
$\frac{1}{4}(0,3,-1)$	$(0, f_{ac}^{3,4}\cos\vartheta, f_{ac}^{3,4}\sin\vartheta)$,
$\frac{1}{4}(0,-3,3)$	$(f_a^{3,3}, (f_{ac}^{3,4}+f_{ac}^{3,3})\cos\vartheta,$ $(f_{ac}^{3,4}-f_{ac}^{3,3})\sin\vartheta - f_c^{3,4})$,

where $\vartheta = \tan^{-1}(c/a)$; so, $\sum_{\vec{r}}$ in Eq. (22) indicates summation over the sites described above.

B. Fourier-transformed Green's function $\tilde{G}_{ij}(\vec{q})$

The Fourier-transformed Green's function for a tetragonal elastic continuum is obtained in a similar way to that followed by Dederichs *et al.* for a cubic lattice[40]

$$\begin{aligned} \tilde{G}_{ij}(\vec{q}) &= \frac{-1}{q^2}\frac{1}{h}K_iK_j\left[\frac{1}{a_ia_j} + (\delta_{j2}\delta_{j2}+\delta_{i2}\delta_{j1})\left(1-\frac{g}{h}\right)\frac{K_3^2}{a_1a_2a_3}\right] \\ &\times\left[1+\sum_n^3\frac{K_n^2}{a_n}+\left(1+\frac{g}{h}\right)\frac{K_3^2}{a_3}\left(\frac{K_1^2}{a_1}+\frac{K_2^2}{a_2}\right)\right]^{-1} \quad (i\neq j), \end{aligned}$$

$$\begin{aligned} \tilde{G}_{ij}(\vec{q}) &= \frac{1}{q^2}\left[\frac{1}{h}-\left(\frac{1}{h}-\frac{1}{g}\right)\delta_{i3}\right]\frac{1}{a_i}\left[1+\sum_n^3\left(\frac{K_n^2}{a_n}\right)-\frac{K_i^2}{a_i}+(1-\delta_{i3})\left(1-\frac{g}{h}\right)\left(\frac{K_1^2K_2^2K_3^2}{a_1a_2a_3}\right)\left(\frac{a_i}{K_i^2}\right)\right] \\ &\times\left[1+\sum_n^3\frac{K_n^2}{a_n}+\left(1+\frac{g}{h}\right)\frac{K_3^2}{a_3}\left(\frac{K_1^2}{a_1}+\frac{K_2^2}{a_2}\right)\right]^{-1} \quad (i=j), \end{aligned}$$

with

$$\begin{aligned} &h = C_{12}+C_{66}, \quad g = C_{13}+C_{44}, \\ &a_i = (1/h)[(C_{11}-C_{12}-2C_{66})K_i^2 \\ &\qquad +(C_{44}-C_{66})K_3^2+C_{66}] \quad (i\neq 3), \\ &a_3 = (1/g)[C_{33}-C_{13}-2C_{44})K_3^2+C_{44}], \end{aligned} \tag{23}$$

where the K_i are the direct cosines (q_i/q) of $\vec{q}$, and δ_{ij} is the Kronecker delta.

In calculating the strain energy and the relaxation energy, we have employed the elastic constants obtained by Fritz[41] and the following ionic radii for O^{2-} and Ti^{4+} ions[42]:

$$C_{11} = 2.701, \quad C_{33} = 4.819, \quad C_{44} = 1.239,$$

$$C_{66} = 1.930, \quad C_{12} = 1.766, \quad C_{13} = 1.480,$$

in units of 10^{12} dyn/cm^2,

$$r_O = 1.40\ \text{Å}, \quad r_{Ti} = 0.605\ \text{Å}.$$

where r_O and r_{Ti} are the ionic radii of O^{2-} and Ti^{4+}, respectively.

We have used a computer to evaluate the strain energy and the relaxation energy because of the algebraic complexity of the terms; no approximation is involved.

C. Results

First, we have calculated the strain energy and the relaxation energy per unit area per plane in the array $(U_S)_A$ and $(U_R)_A$, respectively, and plotted the total energy U_A, the sum of $(U_S)_A$ and $-(U_R)_A$, as a function of n in Fig. 6. The striking feature is that U_A decreases only a little in both cases of {132} and {121} CS planes as n increases, but the curves are oscillatory, i.e., they have series of peaks and valleys. For {132} CS planes, their valleys occur at $n=7$, 10, 13, 16, 19, 22, ..., i.e., $\Delta n = 3$, and in the {121} case the valleys are at n *odd*. In the strain energy of $\{10m\}$ CS planes in reduced WO_3 crystals,[17,43] a similar series of peaks and valleys is also observed. Thus, these must be general properties of the crystal of interest, and not specific to the discrete defect forces we have taken. In both cases of {132} and {121} CS planes, $(U_S)_A$ and $-(U_R)_A$ decrease as n increases and oscillate as a function of n with the same periodicity shown in Fig. 6. We have employed the continuum approximation for the Green's function and the discrete approximation for $F(\vec{q})$, but one could envisage a situation in which the oscillations on the curves in Fig. 6 might disappear if the continuum approximation for $F(\vec{q})$ were made. On the other hand, the $(U_R)_A$ values are found to be always negative in both the {132} and {121} cases. This may be due to the fact that every cation in a CS plane is attracted to the inside of the CS plane by all other forces in that CS plane. The variation of U_A with change of n is small, which means that surrounding CS planes in the ordered array contribute to U_A only slightly compared with the contribution from the CS plane in which we have chosen the origin of the coordinates.

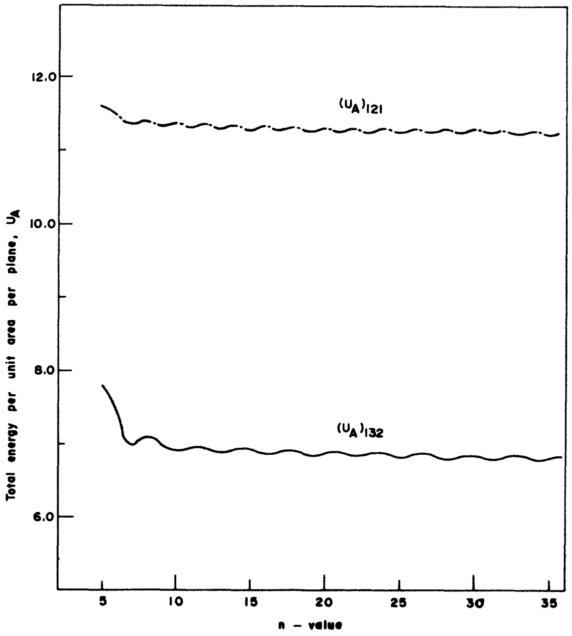

FIG. 6. Total shear-plane energies U_A per unit area per CS plane in infinite ordered arrays of {132} and {121} CS planes as a function of n in Ti_nO_{2n-1}. Shear-plane energies are plotted in arbitrary units.

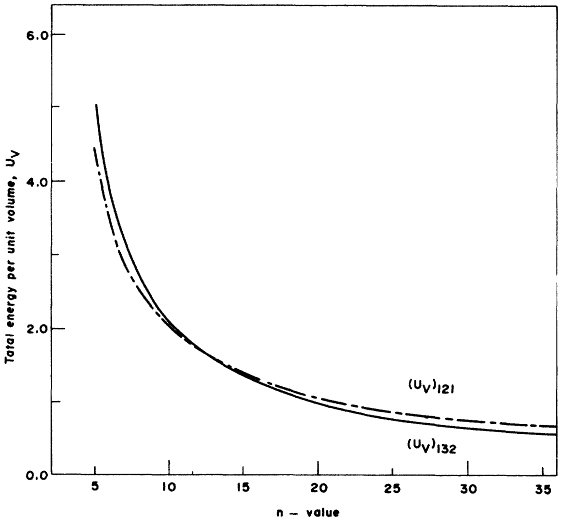

FIG. 7. Total shear plane energies U_V per unit volume in infinite ordered arrays of {132} and {121} CS planes as a function of n. The energies are plotted in arbitrary units.

Though U_A in the ordered {132} array is always lower than for the {121} in the region of $n=5$ to 36, we must determine the energy per unit volume in the ordered array so as to clarify which type of CS plane, {132} or {121}, is more stable for the composition Ti_nO_{2n-1}. We have reduced $(U_S)_A$ and $(U_R)_A$ to the strain energy and the relaxation energy per unit volume, $(U_S)_V$ and $(U_R)_V$, and plotted the total energy per unit volume, i.e., $U_V = (U_S)_V - (U_R)_V$, of a member of the infinite periodic array as a function of n in Fig. 7. In both the {132} and {121} cases U_V falls off smoothly with increasing n and the peaks and valleys clearly recognizable in Fig. 6 seem to disappear because the spacing between CS planes increases much more rapidly than the change in U_A as n increases. The main feature in Fig. 7 is that there is a crossover in the energy curves and the difference between these values increases as n increases beyond $n=11$ or decreases below $n=10$.

According to the constant terms used in Eqs. (8) and (9), one unit on the vertical axis in Fig. 6 corresponds to 0.063 eV/Å^2 and one unit on the vertical axis in Fig. 7 corresponds to 0.021 eV/Å^3.

IV. DISCUSSION

The quantitative results in this paper predict several important features which can be compared with experimental results.

A. Formation energy of isolated CS planes

First, we can estimate the formation energy of a CS plane from Fig. 6. This figure suggests that the U_A values of {132} and {121} CS planes are expected to converge to some constant value at high n values, which means that the U_A values at $n=\infty$ are insensitive to the interaction due to surrounding CS planes. Then, if an isolated CS plane is introduced into a crystal, the increase in energy per unit area of the CS plane is equivalent to the U_A value extrapolated at $n=\infty$ in Fig. 6, and this can be defined as the formation energy (U_f) for that CS-plane type. The ratio of the formation energy of a {121} CS plane $(U_f)_{121}$, to that of a {132} plane, $(U_f)_{132}$, is then estimated to be $[(U_f)_{121}/(U_f)_{132}]\simeq 1.6$. In addition to the formation energy due to the strain, the dissociation energy of oxygen ions must be considered when a CS plane is formed in a single crystal.[19,44] Two oxygen ions per $a^2[1+5(c/a)^2]^{1/2}$ area in the case of a {121} CS plane, and two per $a^2[4+10(c/a)^2]^{1/2}$ area in the case of a {132} CS plane are to be eliminated. So the dissociation energy of oxygen ions per unit area of a CS plane U_d can be written as follows[19,44]:

$$(U_d)_{132}=2E_f/a^2[4+10(c/a)^2]^{1/2}, \qquad (24a)$$

$$(U_d)_{121}=2E_f/a^2[1+5(c/a)^2]^{1/2}, \qquad (24b)$$

or

$$(U_d)_{132}=2E_{\mathrm{bond}}(\mathrm{Ti-O})/a^2[4+10(c/a)^2]^{1/2}, \qquad (24c)$$

$$(U_d)_{121}=2E_{\mathrm{bond}}(\mathrm{Ti-O})/a^2[1+5(c/a)^2]^{1/2}, \qquad (24d)$$

where E_f is the formation energy of an oxygen vacancy and E_{bond} (Ti – O) is the Ti-O binding energy. This yields the relation

$$(U_d)_{121}/(U_d)_{132}=1.628\,.$$

These results show that a {132} CS plane is much more likely to form in a single crystal of rutile than a {121} CS plane. Thus the difference in energy of isolated {132} and {121} planes clarifies the experimental result that {132} CS planes are formed firstly in rutile when the degree of reduction is small.

B. Change of CS plane type

The result in Fig. 7 also agrees very well with the observed change from {132} to {121} shear planes as the oxygen deficiency is increased. Figure 7 indicates that, in the region of $n\leq 10$, $(U_V)_{121}$ is less than $(U_V)_{132}$. This result suggests that ordered {121} arrays must be formed instead of {132} arrays when x in TiO_x is less than 1.90, which coincides with the results in Refs. 7 and 11–13. In the region of $n\geq 11$, $(U_V)_{132}$ is less than $(U_V)_{121}$, but the difference between them becomes appreciable only at n values greater than 16. This result suggests that a {132} array is preferred when x is greater than 1.94, in good agreement with the experimental observations that in the region of $x=1.93$–1.98, ordered arrays of {132} CS planes with the n values of 16–36 are formed. According to the result in Fig. 7, although $(U_V)_{132}$ is less than $(U_V)_{121}$ in the region of $n=11$–15, their difference is so small that we can not recognize it clearly. It is of interest that, in this region, swinging CS planes are observed experimentally.

At small degrees of reduction, the energy of the isolated plane is the dominant factor, but as the reduction is increased, the interaction energy between planes becomes more important. Here it should be noted that we could not have such a good correlation between our theory and experiments in the case of reduced rutile if we were to omit either $(U_S)_V$ or $(U_R)_V$ as shown in Fig. 7. Both of these factors are necessary in the quantitative analysis of the observations of reduced rutile CS structures.

C. Stability of homologous oxides

Within any one family of CS planes, it has been found empirically that some homologs, those with *n even* in the $\mathrm{Ti}_n\mathrm{O}_{2n-1}$ series based upon the ordered {132} CS phase, for example, are favored over those with *n odd*. In the case of the {121} CS phase, a similar behavior has not been established because "two-phase" mixtures are, in the main, observed. In {132} CS phases, some members of a series are likely to be thermodynamically more stable than others. To explain this, imagine a crystal of the oxide $\mathrm{Ti}_n\mathrm{O}_{2n-1}$ to contain an ordered array of {132} or {121} CS planes. Simply by redistributing the CS planes laterally, we can formally convert the original crystal into a crystal containing two phases, $\mathrm{Ti}_{n_1}\mathrm{O}_{2n_1-1}$ and $\mathrm{Ti}_{n_2}\mathrm{O}_{2n_2-1}$, which are distributed alternately as shown in Fig. 8 without changing the total number of CS planes, that is,

$$2\mathrm{Ti}_n\mathrm{O}_{2n-1}=\mathrm{Ti}_{n_1}\mathrm{O}_{2n_1-1}+\mathrm{Ti}_{n_2}\mathrm{O}_{2n_2-1}\,. \qquad (25)$$

Although there are plenty of combinations of n_1 and n_2 which are subject to the condition of Eq. (25), it is impractical to calculate all the combinations and, as indicated in Fig. 8, we have only

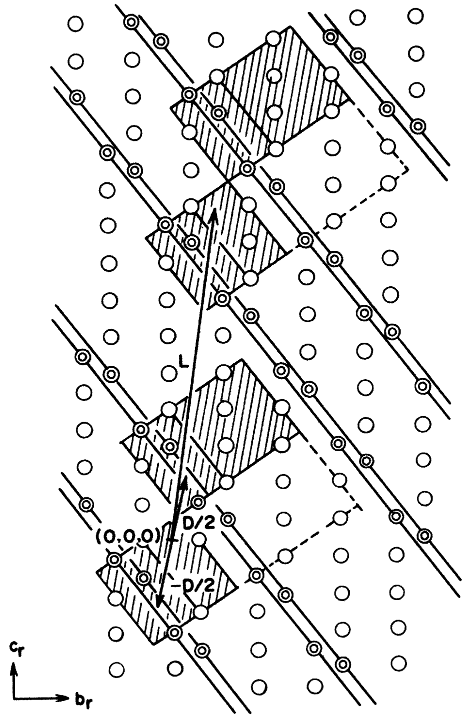

FIG. 8. Ti sites on (100) in a crystal containing two phases Ti_5O_9 and Ti_7O_{13} based upon {121} CS. Though formal periodic unit cells are indicated by broken lines, the periodic unit cell employed in the calculations consists of two regions (shaded parts), one is the unit cell of the Ti_5O_9 oxide and the other is that of Ti_7O_{13}. The origin of the coordinates in the "two-phase" mixture is taken to be midway along the vector $\vec{D}$ from the origin of the Ti_5O_9 unit cell to the origin of the Ti_7O_{13} unit cell.

employed the pair $n_1 = n - 1$ and $n_2 = n + 1$ as did Iguchi and Tilley.[17] The theoretical treatment is quite the same as for an infinite ordered array except for the following points. The vectors $\vec{A}$ and $\vec{B}$ are the same ones as in Eq. (1), but $\vec{C}$ is expressed as follows for {132} and {121} CS planes:

$$\begin{aligned} &\vec{C} = d'(\vec{b} + \vec{c}), \\ &d' = \tfrac{4}{5}(2n - 1) \text{ for } \{132\} \text{ CS}, \\ &d' = \tfrac{4}{3}(2n - 1) \text{ for } \{121\} \text{ CS}. \end{aligned} \tag{26}$$

The vector $\vec{L}$ in the translation vector $\vec{T}$ is (see Fig. 8)

$$\begin{aligned} &\vec{L} = 4(\delta\vec{b} + 2L\vec{c}), \\ &\left.\begin{aligned} &\delta = (-1)^n \\ &L = \begin{cases} \tfrac{1}{2}(n-2), & n \text{ even} \\ \tfrac{1}{2}(n+1), & n \text{ odd} \end{cases} \end{aligned}\right\} \text{ for } \{132\} \text{ CS}, \\ &\delta = 1, \; L = \tfrac{1}{2}(2n - 3) \text{ for } \{121\} \text{ CS}. \end{aligned} \tag{27}$$

For crystals containing the mixed oxides, $Ti_{n-1}O_{2(n-1)-1}$ and $Ti_{n+1}O_{2(n+1)-1}$, the Fourier-transformed force $\tilde{F}_{mix}(\vec{q})$ can be obtained in a similar way as in the calculation for a pair of CS planes by Stoneham *et al.*[16] As shown in Fig. 8, we have chosen the origin of the coordinates in the "two-phase" mixture to be midway along the vector $\vec{D}$, from the origin of the unit cell of $Ti_{n-1}O_{2(n-1)-1}$ to that of the unit cell of $Ti_{n+1}O_{2(n+1)-1}$. Then $\tilde{F}_{mix}(\vec{q})$ has the form

$$\begin{aligned} \tilde{F}_{mix}(\vec{q}) &= \sum_{\vec{r} - \vec{D}/2} F(\vec{r} - \tfrac{1}{2}\vec{D}) e^{i\vec{q}\cdot(\vec{r} - \vec{D}/2)} \\ &\quad + \sum_{\vec{r} + \vec{D}/2} F(\vec{r} + \tfrac{1}{2}\vec{D}) e^{i\vec{q}\cdot(\vec{r} + \vec{D}/2)} \\ &= 2\cos(\vec{q} \cdot \tfrac{1}{2}\vec{D}) \tilde{F}(\vec{q}), \end{aligned} \tag{28}$$

where $\tilde{F}(\vec{q})$ is the same one as in Eq. (22) and $\vec{D}$ has the following form:

$$\begin{aligned} &\vec{D} = 2(\delta\vec{b} + 2L\vec{c}), \\ &\delta = (-1)^n, \\ &L = \left\{\begin{aligned} &\tfrac{1}{2}(n-3), \quad n \textit{ even} \\ &\tfrac{1}{2}n, \quad n \textit{ odd} \end{aligned}\right\} \text{ for } \{132\} \text{ CS}, \\ &\left.\begin{aligned} &\delta = 1 \\ &L = \tfrac{1}{2}(n-5) \end{aligned}\right\} \text{ for } \{121\} \text{ CS}. \end{aligned} \tag{29}$$

Using these relations, we have calculated the energy per unit volume of the "two-phase" mixture, which is denoted as $(U_{mix})_V$. The difference in energy per unit volume $(\Delta U)_V = (U)_V - (U_{mix})_V$ is shown in Fig. 9 as a function of n. If $(\Delta U)_V$ is negative the Ti_nO_{2n-1} oxide will be stable, while if $(\Delta U)_V$ is positive the phase will be disproportionate with respect to the phases on either side. As seen in Fig. 9, it is clear that $(\Delta U)_V$ of the {132} phase has a series of maxima and minima with a periodicity $\Delta n = 3$ while, in the {121} case ordered arrays of $n = 5, 7, 9, 11, \ldots$ are favored, i.e., $\Delta n = 2$. It is of interest that the valleys of $(U)_A$ in Fig. 6 occur at these stable n values in Fig. 9. In order to confirm this correlation, we have calculated $(U_{mix})_V$ for several combinations of n_1 and n_2 when $n = 16$, which is expected to be one of the most stable n value of the ordered {132} array observed in practice, and we have plotted $(U_{mix})_V$ for these combinations in Fig. 10. This result demonstrates clearly that the combinations of n_1 and n_2 at which the valleys of $(U)_A$ occur in Fig. 6 correspond to minima of $(U_{mix})_V$ values.

According to our results, homologs with $n = 13, 16, 19, 22, \ldots$ in the Ti_nO_{2n-1} series based upon ordered {132} CS planes may be stable. However, in most of the specimens investigated by Bursill and Hyde[9] ordered arrays of {132} CS planes with n values of 16, 18, 20, and 22 are mainly observed

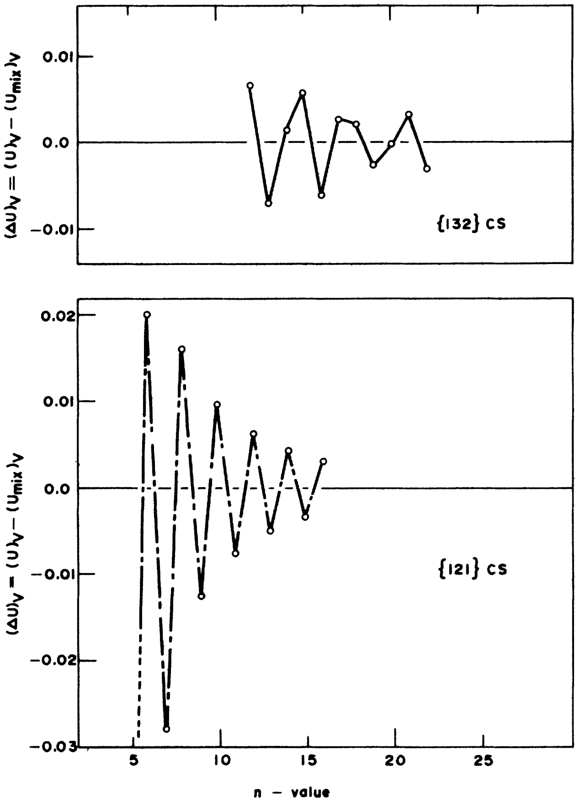

FIG. 9. Difference between $(U)_V$ and $(U_{\mathrm{mix}})_V$ as a function of n. $(U)_V$ is the shear-plane energy in an infinite array of $\mathrm{Ti}_n\mathrm{O}_{2n-1}$ and $(U_{\mathrm{mix}})_V$ represents the energy of a crystal containing two phases $\mathrm{Ti}_{(n-1)}\mathrm{O}_{2(n-1)-1}$ and $\mathrm{Ti}_{(n+1)}\mathrm{O}_{2(n+1)-1}$. The units of the vertical axis are arbitrary.

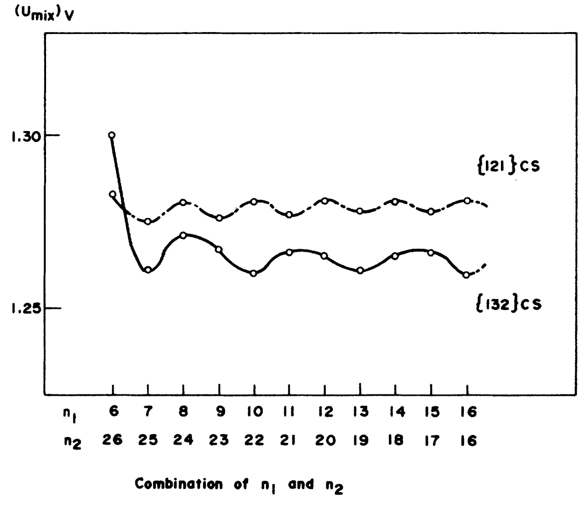

FIG. 10. $(U_{\mathrm{mix}})_V$ for several combinations of n_1 and n_2 when $n=16$. The vertical axis represents $(U_{\mathrm{mix}})_V$ in arbitrary units and the horizontal axis indicates the combination of n_1 and n_2.

and homologs with other n values are rarely identified. Moreover, Terasaki and Watanabe found a "two-phase" mixture of {132} CS planes with n values of 13 and 14.[13] Thus some features observed experimentally agree with our calculation, but some deviate slightly from our theory. Our prediction, however, presupposes that the specimen is in thermal equilibrium. It should be noted that, even in WO_3 samples doped with a few percent of germanium at 1100 °C for 5 weeks during preparation, the perfect-equilibrium state was not apparently obtained.[45] One would, therefore, expect that CS-plane microstructures could well be sensitive to both heating times and heating temperatures during preparation.

In the case of {121} CS planes, the homologs with *n odd* seem to be stable theoretically and these arrays are expected to be observed if the sample is in thermal equilibrium, although "two-phase" mixtures are detected in practice. In addition, the lattice polarization also seems to be one of the factors which should be considered in understanding the stability of homologous oxides, but this may require a formidable calculation. In order to establish a more accurate correlation between the experimental results and our theory, careful statistical surveys of experimental results equivalent to that for {103} CS planes in reduced WO_3 shown in the previous work[17] would be helpful.

D. Nature of CS planes

We have tried the following related models of the defect forces. One consists in estimating the ratio of the forces by assuming the total positive charge in the CS plane to be distributed equally over all the cations in the CS plane, making the valence state of a cation in the {132} or {121} CS plane either $+\frac{11}{3}e$ or $+\frac{7}{2}e$. A second alternative is obtained by considering only the Born-Mayer potential, the second term on the right-hand side of Eq. (8). A third alternative may be obtained by omitting the dielectric constant ϵ in Eq. (8) because the interaction between cations in the CS plane could possibly be regarded to be of short range. However, the results calculated by using these ratios were quite similar to that reported above and will not be considered further here.

There still remains the question of whether the CS-plane regions can be treated as elastic continua the same as the matrix. Although the force is assumed to be transmitted through the CS planes without any damping, in this report, Iguchi and Tilley[17] hypothesized that the force can not pass through the CS plane in WO_{3-x}. In experimental results, the cumulative outcome that the CS plane spacings near the center in a cluster are close is certainly found for TiO_{2-x},[14] but such an outcome has not been found for WO_{3-x} up to date. This shows the difference in the nature of the CS planes in TiO_{2-x} and WO_{3-x}. This problem will be another project.

In this paper we have used the idealized rutile structure. This model explains the experimental observations very well while, on the other hand, the real structure may need a complicated and long calculation. Thus the results presented in this paper suggest that the strain energy is one of the most important factors in controlling the observed microstructures.

ACKNOWLEDGMENTS

The authors are indebted to Dr. S. Kurita, Dr. A. M. Stoneham, Dr. R. J. D. Tilley, and Professor J. S. Anderson for many useful discussions. They are also indebted to Professor R. Wada for his encouragement during the course of this work.

---

[1] As a review, see F. A. Grant, Rev. Mod. Phys. 31, 646 (1959).

[2] P. F. Chester, J. Appl. Phys. 32, 2233 (1961).

[3] J. H. Becher and W. R. Hosler, J. Phys. Soc. Jpn. II, 152 (1963).

[4] J. B. Wachtman, Jr. and L. R. Doyle, Phys. Rev. 135, 276 (1964).

[5] E. Iguchi and K.Yajima, J. Phys. Soc. Jpn. 32, 1415 (1972).

[6] J-H. Baumard and F. Gerrais, Phys. Rev. B 15, 2316 (1977).

[7] S. Andersson, B. Cóllen, U. Kuylenstierna, and A. Magñeli, Acta.Chem. Scand. 11, 1641 (1957).

[8] L. A. Bursill, B. G. Hyde, O. Terasaki, and D. Watanabe, Philos. Mag. 23, 347 (1969).

[9] L. A. Bursill and B. G. Hyde, Acta Crystallogr. B 27, 210 (1971).

[10] S. Andersson, B. Cóllen, G. Kruse, U. Kuylenstierna, A. Magnéli, H. Pestmalis, and S. Åsbrink, Acta Chem. Scand. 11, 1653 (1957).

[11] S. Andersson, Acta Chem. Scand. 14, 1161 (1960).

[12] S. Andersson and L. Jahnberg, Ark. Kemi. 21, 413 (1963).

[13] O. Terasaki and D. Watanabe, J. Phys. Soc. Jpn. 10, 292 (1971).

[14] L. A. Bursill and B. G. Hyde, *Progress in Solid-State Chemistry*, edited by H. Reiss and J. O. McCaldin (Pergamon, Oxford, 1972), Vol. 7, p. 177.

[15] L. A. Bursill and B. G. Hyde, Philos. Mag. 23, 3 (1971).

[16] A. M. Stoneham and P. J. Durham, J. Phys. Chem. Solids 34, 2127 (1973).

[17] E. Iguchi and R. J. D. Tilley, Philos. Trans. R. Soc. Lond. A 286, 55 (1977).

[18] E. Iguchi and R. J. D. Tilley, J. Solid State Chem. 21, 49 (1977).

[19] E. Iguchi, J. Phys. Chem. Solids 38, 1039 (1977).

[20] P. Clapp, *The Chemistry of Extended Defect in Non-Metallic Solids*, edited by L. Eyring and M. O'Keeffe (North-Holland, Amsterdam, 1970), p. 663.

[21] G. J. Dienes, D. O. Welch, C. R. Fischer, R. D. Hatcher, O. Lazareth, and M. Samberg, Phys. Rev. B 11, 3060 (1975).

[22] C. R. A. Catlow, Proc. R. Soc. Lond. A 353, 533 (1977).

[23] H. Kanzaki, Phys. Chem. Solids 2, 24 (1957).

[24] A. G. Khachaturyan, Sov. Phys.-Solid State 9, 2249 (1968).

[25] H. Cook and D. de Fontaine, Acta Met. 17, 915 (1969).

[26] D. W. Hoffman, Acta Met. 18, 819 (1970).

[27] J. S. Anderson, in Ref. 20, p. 14.

[28] J. Yamashita, J. Phys. Soc. Jpn. 9, 339 (1954).

[29] J. Yamashita and T. Kurosawa, J. Phys. Soc. Jpn. 9, 944 (1954).

[30] J. Yamashita and T. Kurosawa, J. Phys. Soc. Jpn. 10, 610 (1955).

[31] R. Wyckoff, *Crystal Structures* (Interscience, New York, 1963), Vol. I.

[32] W. H. Baur, Acta Crystallogr. 9, 515 (1956).

[33] J. S. Anderson and B. G. Hyde, J. Phys. Chem. Solids, 28, 1393 (1967).

[34] B. A. DeAnglis and M. Schiavello, J. Solid State Chem. 21, 67 (1977).

[35] L. Pauling, *The Nature of Chemical Bond* (Cornell U. P., Ithaca, N. Y., 1960), p. 505.

[36] I. L. Torrens, *Interatomic Potentials* (Academic, New York, 1972), p. 229.

[37] G. A. Samara and P. S. Peercy, Phys. Rev. B 7, 1131 (1973).

[38] H. B. Huntington, *Solid State Physics*, edited by F. Seitz and D. Turnbull (Academic, New York, 1971), Vol. 17, p. 216.

[39] J. P. Hirth and J. Lothe, *Theory of Dislocation* (McGraw-Hill, New York, 1968), p. 29.

[40] P. H. Dederichs and G. Leibfried, Phys. Rev. 188, 1175 (1969).

[41] I. J. Fritz, J. Phys. Chem. Solids, 35, 817 (1974).

[42] R. D. Shannon and R. J. Prexitt, Acta Crystallogr. B 25, 925 (1973).

[43] E. Iguchi and R. J. D. Tilley, J. Solid State Chem. (to be published).

[44] R. J. D. Tilley, J. Solid State Chem. 19, 53 (1976).

[45] E. Iguchi and R. J. D. Tilley (unpublished data).